

Mature induced-pluripotent-stem-cell-derived human podocytes reconstitute kidney glomerular-capillary-wall function on a chip

Samira Musah^{1,2,3}, Akiko Mammoto⁴, Thomas C. Ferrante¹, Sauveur S. F. Jeanty¹, Mariko Hirano-Kobayashi^{1,4}, Tadanori Mammoto⁴, Kristen Roberts¹, Seyoon Chung¹, Richard Novak¹, Miles Ingram¹, Tohid Fatanat-Didar¹, Sandeep Koshy¹, James C. Weaver¹, George M. Church^{1,2,3} and Donald E. Ingber^{1,3,4,5*}

An *in vitro* model of the human kidney glomerulus—the major site of blood filtration—could facilitate drug discovery and illuminate kidney-disease mechanisms. Microfluidic organ-on-a-chip technology has been used to model the human proximal tubule, yet a kidney-glomerulus-on-a-chip has not been possible because of the lack of functional human podocytes—the cells that regulate selective permeability in the glomerulus. Here, we demonstrate an efficient (over 90%) and chemically defined method for directing the differentiation of human induced pluripotent stem (hiPS) cells into podocytes that express markers for a mature phenotype (nephrin⁺, WT1⁺, podocin⁺, PAX2⁻) and that exhibit primary and secondary foot processes. We also show that the hiPS-cell-derived podocytes produce glomerular basement-membrane collagen and recapitulate the natural tissue-tissue interface of the glomerulus, as well as the differential clearance of albumin and inulin, when co-cultured with human glomerular endothelial cells in an organ-on-a-chip microfluidic device. The glomerulus-on-a-chip also mimics adriamycin-induced albuminuria and podocyte injury. This *in vitro* model of human glomerular function with mature human podocytes may facilitate drug development and personalized-medicine applications.

One of the most essential functional units of the kidney is the glomerulus—the network of capillaries through which circulating blood gets filtered into urine¹. Glomerular capillaries are lined by endothelial cells and encased by podocytes, a highly differentiated epithelial cell type that constitutes a major proportion of the kidney filtration barrier by regulating selective filtration across the capillary wall that separates the blood and urinary spaces². Indeed, most acquired and hereditary forms of glomerular disease, as well as some drug toxicities, are characterized by podocyte loss or dysfunction, which results in proteinuria and nephron degeneration³. The ability to develop *in vitro* models that recapitulate human glomerular function would greatly help to advance our understanding of the mechanisms that underlie kidney development and facilitate the establishment of disease models to guide therapeutic discovery⁴. Unfortunately, efforts to develop *in vitro* models of the human glomerulus have been held back by the lack of functional human kidney podocytes.

hiPS cells have a remarkable capacity to self-renew indefinitely and differentiate into almost any cell type under appropriate conditions^{5,6}. hiPS cells could potentially serve as an unlimited source of podocytes. Indeed, there has been increasing effort to derive podocytes from hiPS cells. However, a method for directing their differentiation specifically into podocytes, free of other cell types, with high efficiency remains unknown. Previous attempts to derive podocytes from hiPS cells have been promising, however, these attempts have relied on nonspecific differentiation through embryoid body

formation⁷ or co-culture with animal tissues and serum components^{8,9}. But the embryoid body differentiation method produces cells that simultaneously differentiate into multiple lineages and is therefore limited by high levels of heterogeneity, poor reproducibility and an inability to generate mature podocytes that are isolated free from other cell types. Organoids, which offer another notable approach for the study of tissue differentiation, also have been formed from nephron-like progenitor cells. Although this method is noteworthy, it has limitations regarding the ability to replicate glomerular-specific functions probably owing to the complication of low numbers of immature nephron-like cells and the presence of a highly heterogeneous cell population including non-nephrogenic derivatives^{10,11}. In addition to lacking cell lineage specificity, kidney organoids also have limited control over tissue structure and function, and fail to form a functional endothelium-lined vascular circuit that is necessary for glomerular filtration studies. Therefore, it remains unclear which signals within the cellular microenvironment contribute specifically to podocyte lineage specification and maturation, and as a result there is still no practical source of pure populations of mature, functional, kidney glomerular podocytes available for the development of *in vitro* models of human kidney glomerular function.

Here we show that simultaneous modulation of a few signalling pathways that have been implicated in glomerular development enables the rapid and efficient lineage conversion of hiPS-cell derivatives into terminally differentiated cells that exhibit morphological,

¹Wyss Institute for Biologically Inspired Engineering, Harvard University, Boston, Massachusetts 02115, USA. ²Department of Genetics, Harvard Medical School, Boston, Massachusetts 02115, USA. ³Harvard Stem Cell Institute, Harvard University, Cambridge, Massachusetts 02138, USA. ⁴Vascular Biology Program, Children's Hospital and Harvard Medical School, Boston, Massachusetts 02115, USA. ⁵Harvard John A. Paulson School of Engineering and Applied Sciences, Harvard University, Cambridge, Massachusetts 02139, USA. *e-mail: don.ingber@wyss.harvard.edu

molecular and functional characteristics of mature kidney glomerular podocytes. By co-culturing the hiPS-cell-derived podocytes with a layer of human kidney glomerular endothelium in an organ-on-a-chip microfluidic device, we also developed a functional microfluidic device that mimics the tissue–tissue interface and molecular filtration properties of the glomerular capillary wall and recapitulates drug-induced podocyte injury and proteinuria *in vitro*. This human glomerulus-on-a-chip could offer a new way to study kidney glomerular function, renal toxicity and mechanisms of kidney disease *in vitro*.

Directed differentiation of hiPS cells into podocytes

Although it remains challenging to restrict pluripotent-stem-cell differentiation into specific cell types in a robust manner, there is increasing evidence that multiple factors within the tissue micro-environment, including cell–cell interactions, timing of exposure to soluble growth factors and physicochemical properties of the extracellular matrix (ECM) can affect stem-cell fate decisions^{12–18}. We therefore explored whether chemically defined soluble factors and insoluble ECM signals can promote the differentiation of hiPS cells into mature podocytes. To avoid the inherent heterogeneity associated with embryoid body differentiation methods and to develop a method more easily integrated with microfluidic organ-on-a-chip technology, we chose to use adherent cell monolayer cultures. Because both hiPS cells¹⁹ and human glomerular podocytes²⁰ express high levels of $\beta 1$ integrin receptor (Supplementary Fig. 1a), we reasoned that ECM proteins that facilitate cell adhesion through engagement of this receptor could serve as suitable matrices to support anchorage of hiPS cells and their transition into podocytes.

Laminins are widely expressed in the glomerular basement membrane (GBM) during development and functional maturation of the kidney^{21,22} and integrin signalling has a notable role in the maintenance of glomerular structure and filtration^{23,24}. We therefore examined surfaces functionalized with laminin-511, laminin-511 E8 fragment, laminin-521 or type I collagen (as a control) for their ability to support hiPS-cell adhesion under serum-free conditions. These studies revealed that whereas hiPS cells only poorly adhered to type I collagen, surfaces coated with laminin-511, laminin-511 E8 fragment or laminin-521 were all effective for the attachment and propagation of dissociated hiPS cells (Supplementary Fig. 1b, c). We used the laminin-511 E8 fragment for all subsequent studies based on its higher cell-binding efficiency and lower cost.

In the embryo, most kidney cells, including glomerular podocytes, develop from the intermediate mesoderm that is, in turn, derived from the mesoderm germ layer²⁵. Following this developmental paradigm (Fig. 1a), we first seeded dissociated hiPS cells and cultured them on tissue-culture plates coated with the laminin-511 E8 fragment in a mesoderm-induction medium containing activin A and a small-molecule activator of canonical Wnt signalling (CHIR99021)²⁶, as well as the Rho-associated kinase (ROCK) inhibitor Y27632 to improve cell survival¹⁴. After two days, the cells displayed nearly homogeneous expression of the mesoderm markers gooseoid, HAND1 and brachyury (Supplementary Fig. 2a, b). To promote differentiation into intermediate mesoderm, the hiPS-cell-derived mesoderm cells were re-fed with medium containing bone morphogenetic protein 7 (BMP7) and CHIR99021, and cultured for a minimum of 14 days. Consistent with a previous report²⁶, this treatment produced cells that expressed the intermediate mesoderm and metanephric nephron progenitor cell markers²⁷, odd-skipped related 1 (OSR1), Wilms tumor 1 (WT1) and PAX2 (Fig. 1a and Supplementary Fig. 2c). We found that the resulting intermediate mesoderm cells undergo proliferation, as measured by incorporation of EdU into DNA (Supplementary Fig. 2c) and can be passaged every 8–12 days for up to 60 days or be successfully cryopreserved. Moreover, similar results were obtained with surfaces functionalized with laminin-511 and laminin-521 (data not

shown). These results indicate that laminin-functionalized surfaces support the ability of soluble inductive factors to promote adhesion of hiPS cells and their directed differentiation into the intermediate mesoderm lineage.

To direct differentiation of hiPS cells into mature podocytes, we developed a novel podocyte-inducing differentiation medium containing soluble factors that have been shown to modulate key signalling pathways involved in glomerular development and podocyte lineage determination *in vivo*, including VEGF (vascular endothelial growth factor), retinoic acid, CHIR99021, BMP7 and activin A (Fig. 1a). Our rationale was as follows. We selected VEGF based on previous genetic and immunological studies showing that VEGF was indispensable for the differentiation of podocytes and growth of glomerular capillaries during kidney development^{28,29}. Retinoic acid signalling induces the expression of the podocyte-specific markers nephrin and WT1 (ref. ³⁰). CHIR99021 is a potent activator of canonical Wnt signalling, which stimulates embryonic nephron progenitors to form glomerular structures³¹. BMP7 promotes the survival of nephrogenic cells during kidney development³². And activin A enhances the expression of nephrogenic genes in the animal cap tissue (multipotential cells around the animal pole of the blastula) when used in conjunction with retinoic acid³³.

hiPS-cell-derived intermediate mesoderm cells treated with this medium rapidly (within 4–5 days) acquired morphological features exhibited by kidney glomerular podocytes, including an arborized cell body with a prominent nucleus and multiple fingerlike cell protrusions (Fig. 1b). The larger size of the hiPS-cell-derived cells obtained by this treatment was similar to the size of an immortalized podocyte cell line that was established previously from human kidney biopsies³⁴ (Fig. 1c, d). Flow cytometry analysis also showed that the hiPS-cell-derived cells expressed the podocyte-specific proteins nephrin and WT1, with a corresponding decrease in the expression of the pluripotency marker OCT4 (Fig. 1e). Notably, this method for podocyte induction was highly efficient as more than 90% of the hiPS-cell-derived podocytes co-expressed nephrin and WT1 (Fig. 1f), which is an order of magnitude more efficient than most methods that have been used to differentiate specialized cell types from hiPS cells³⁵. Gene expression analysis for multiple pluripotency and podocyte markers (*POU5F1*, *PAX2*, *WT1*, *NPHS1* and *NPHS2*) also showed comparable transcriptional profiles between the hiPS-cell-derived podocytes and the immortalized podocyte cell line, although the podocyte gene *NPHS2* (encoding podocin) was expressed at higher levels in the hiPS-cell-derived podocytes. There was also a significant downregulation of the progenitor cell-related gene *PAX2* in the hiPS-cell-derived podocytes relative to the immortalized podocyte cells (Supplementary Fig. 3). In addition, we observed high levels of the nephrin-encoding gene *NPHS1*, but low levels of the nephrin protein in undifferentiated hiPS cells (Fig. 1e, f and Supplementary Fig. 3), which is consistent with previous findings⁷. By contrast, immunofluorescence analysis (Fig. 2a, b), flow cytometry and gene expression studies confirmed that nephrin, as well as WT1 and podocin, were expressed at higher levels in the hiPS-cell-derived podocytes, whereas OSR1 and *PAX2* proteins were absent. Because downregulation of *PAX2* is required for podocyte specialization *in vivo*³⁶, these data suggest that the hiPS-cell-derived podocytes may be developmentally more mature than the podocyte cell line. Additionally, the lack of EdU incorporation in the hiPS-cell-derived podocytes (Fig. 2b) confirmed that these cells were terminally differentiated, as is observed in mature podocytes in functional glomeruli^{21,37}.

As podocytes become more specialized during kidney development, nephrin is shuttled from the nucleus to the cytoplasm and plasma membrane^{38,39}. Therefore, the subcellular localization of nephrin can also indicate the developmental status of podocytes. Immunofluorescence microscopy analysis confirmed that nephrin was more localized in the cytoplasm and on the plasma membrane of the hiPS-cell-derived podocytes compared to the immortalized

podocytes, which exhibited primarily nuclear staining (Fig. 2a). In agreement with this observation, the hiPS-cell-derived podocytes also showed both nuclear and cytoplasmic expression of protein

kinase C lambda/iota (PKC λ /i) (Fig. 2c and Supplementary Fig. 4), which is a cell polarity regulator that maintains the integrity of the glomerular slit diaphragm by trafficking nephrin to the cell

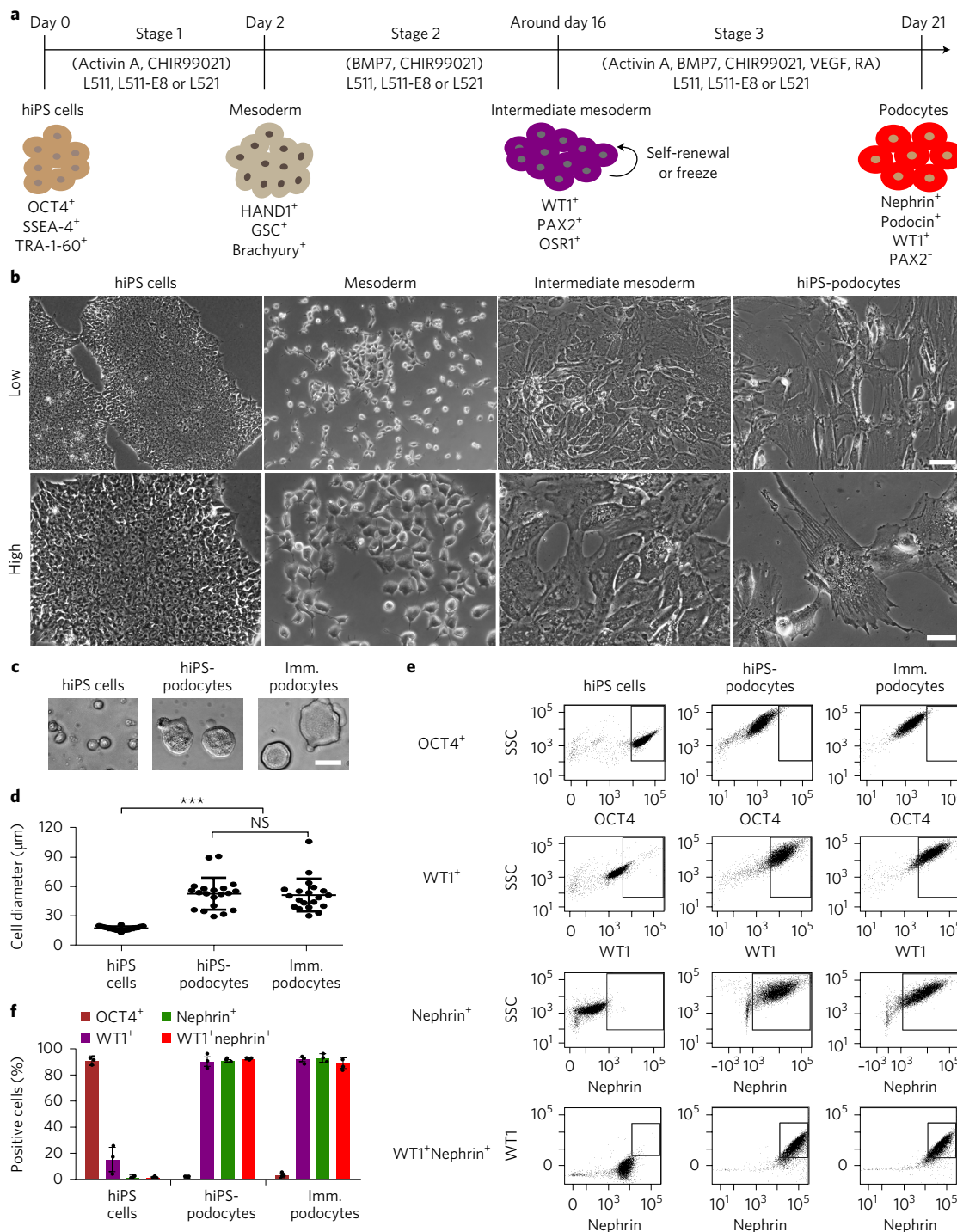


Figure 1 | Efficient differentiation of kidney podocytes from human iPS cells. **a**, Schematic overview of the timeline for directed differentiation of hiPS cells into podocytes. BMP7, bone morphogenetic protein 7; L511, laminin-511; L511-E8, laminin-511-E8 fragment; L521, laminin-521; RA, retinoic acid; VEGF, vascular endothelial growth factor. **b**, Low- and high-magnification bright-field images of cells at each stage of differentiation. hiPS-podocytes, hiPS-cell-derived podocytes. **c**, **d**, Bright-field images (**c**) and scatter plot of the diameter of dissociated (non-adhered) hiPS cells, hiPS-cell-derived podocytes and immortalized (imm.) human podocytes (**d**). **e**, Flow cytometry analysis for the expression of pluripotency and podocyte markers in hiPS cells, hiPS-cell-derived podocytes and immortalized human podocytes. Representative plots showing expression levels of a pluripotency marker (OCT4), kidney cell marker (WT1), nephrin podocyte-specific marker (nephrin) and dual expression of WT1 and nephrin. **f**, Quantitative representation of flow cytometry analysis. The percentage of cells positive for OCT4 (brown), WT1 (purple), nephrin (green) and double positive for WT1 and nephrin (red) is shown. Scale bars, 100 μ m (**b**, top) and 50 μ m (**b**, bottom; **c**). Data are mean \pm s.d.; $n = 20$ cells (**d**) or $n = 3$ independent experiments (**f**); *** $P < 0.0001$; NS, not significant.

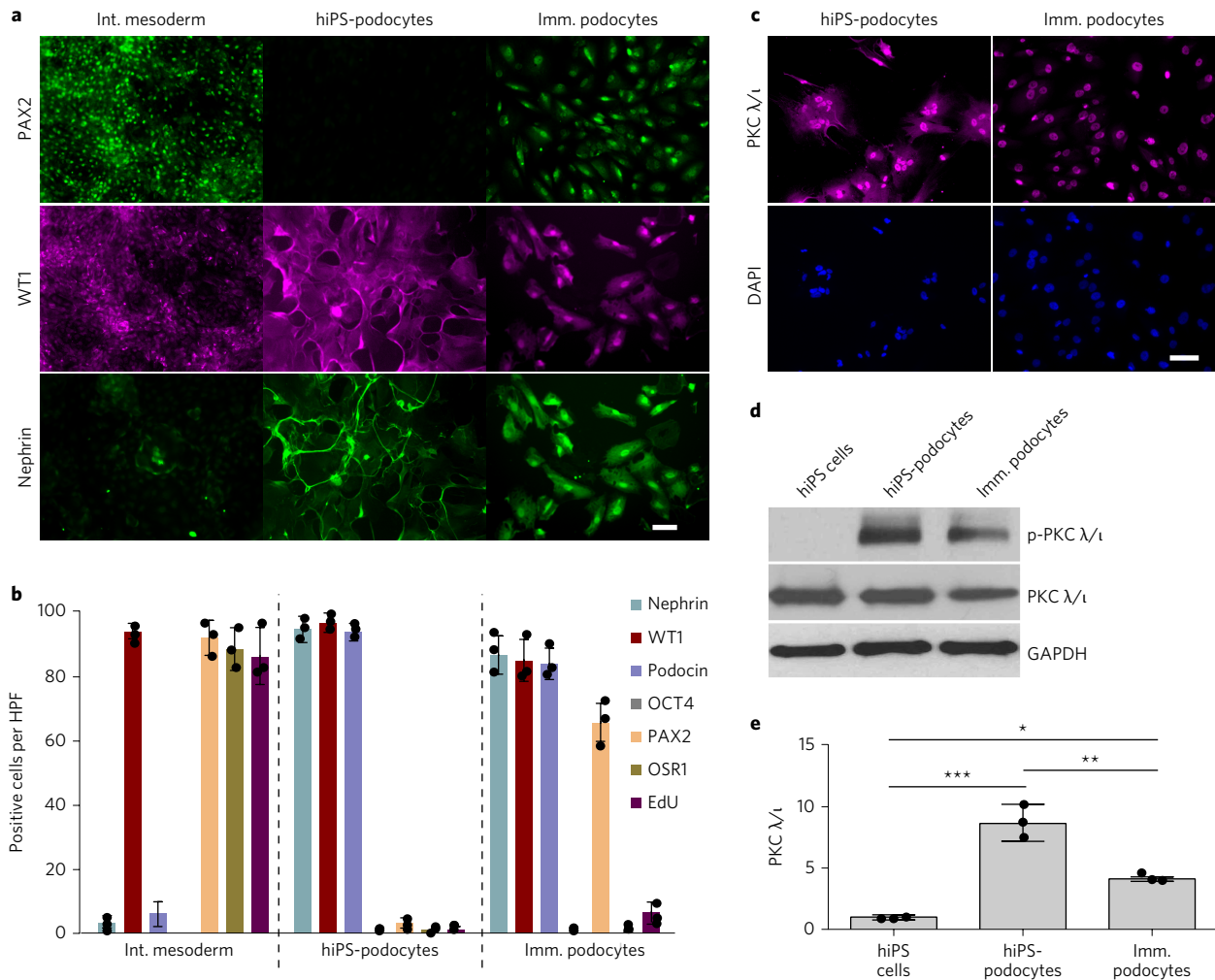


Figure 2 | Human iPS-cell-derived podocytes express markers characteristic of the mature phenotype. a, Representative fluorescence microscopy images of intermediate (int.) mesoderm, hiPS-cell-derived podocytes, and human immortalized podocytes stained for PAX2, WT1 and nephrin. **b**, Quantification of hiPS-cell-derived podocytes indicates upregulation of podocyte markers (nephrin, WT1 and podocin), with a corresponding decrease in the pluripotency marker OCT4. The decrease in progenitor cell markers PAX2 and OSR1, and the lack of EdU incorporation in hiPS-cell-derived podocytes indicate that the cells are post-mitotic and terminally differentiated, similar to mature podocytes. HPF, high-power field; EdU, 5-ethynyl-2'-deoxyuridine; OSR1, odd-skipped related transcription factor protein 1. **c**, Immunofluorescence microscopy images of hiPS-cell-derived podocytes and immortalized human podocytes stained for PKCλ/ι, a putative trafficker of nephrin to cell surface. **d**, Western blot analysis of total and phosphorylated (p-) PKCλ/ι proteins levels in hiPS cells, hiPS-cell-derived podocytes and human immortalized podocytes. **e**, Quantification of phosphorylated PKCλ/ι levels from western blots. Scale bars, 100 μm. Data are mean ± s.d.; *n* = 3 (**b,e**); **P* < 0.05; ***P* < 0.001; ****P* < 0.0001.

surface⁴⁰. The hiPS-cell-derived podocytes also showed enhanced phosphorylation of PKCλ/ι, as determined by western blot analysis (Fig. 2d, e), and deposit basement membrane collagen type IV, as detected by immunofluorescence microscopy (Supplementary Fig. 5). Together, these results show that our differentiation method efficiently produces iPS-cell-derived cells with morphological and molecular phenotypes that are consistent with mature kidney glomerular podocytes. Notably, we found that the podocyte induction method that we used with the PGP1 hiPS cell line used to produce most of the results in this article, can also be used with other hiPS cell lines (IMR-90-1 and IISH3i CB6), as demonstrated by induction of similar characteristic arborized morphology and positive immunoreactivity for podocin (Supplementary Fig. 6a, b).

Differentiation of podocyte morphology and molecular uptake

In the glomerulus, podocytes extend elongated podocin-positive protrusions, known as foot processes, which insert into the GBM, separating the podocytes from the underlying glomerular endothelium and these protrusions have a noteworthy role in the regulation of

glomerular filtration³. Immunofluorescence microscopy analysis showed that although podocin staining was largely limited to the cell body of immortalized podocytes, bright staining was seen in both the cell bodies and narrow membrane protrusions of hiPS-cell-derived podocytes (Fig. 3a, top). Scanning electron microscopy analysis confirmed the presence of both primary and secondary branches in the long cell processes that extended from the hiPS-cell-derived podocytes, whereas these differentiated structures were less developed in the podocyte cell line (Fig. 3a, bottom, and Supplementary Fig. 7a). We also observed that the hiPS-cell-derived podocytes extended their cell processes toward neighbouring cells and form an interconnected multi-cellular network with slit-like spaces between neighbouring cell processes that form tight cell–cell contacts *in vitro* (Supplementary Fig. 7b). These findings are consistent with previous reports that existing human podocyte cell lines do not form well-defined foot processes^{3,41,42}, and by contrast, show that the hiPS-cell-derived podocytes develop structural features that resemble those exhibited by kidney glomerular podocytes *in vivo*²¹.

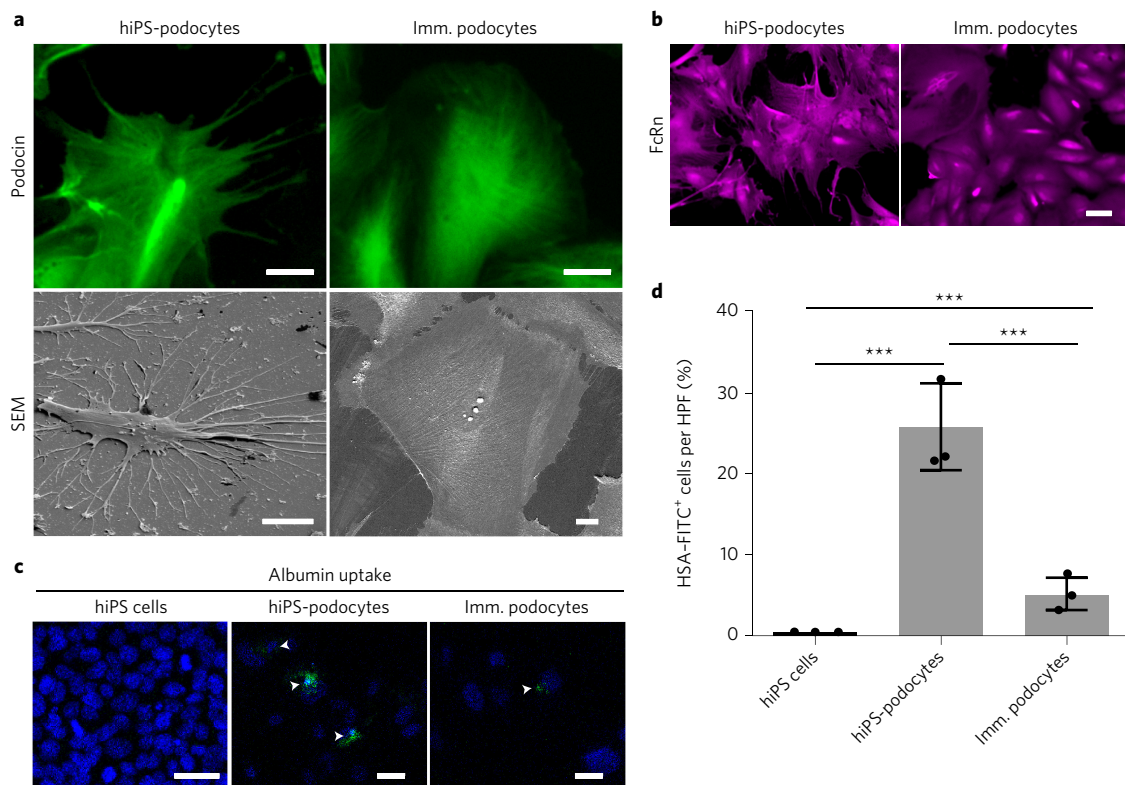


Figure 3 | Human iPS-cell-derived podocytes exhibit primary and secondary cell processes and enhanced molecular uptake of exogenous albumin.

a, Top, fluorescence microscopy images of hiPS-cell-derived podocytes and human immortalized podocytes stained for podocin (green). Bottom, scanning electron microscopy (SEM) images of hiPS-cell-derived podocytes and human immortalized podocytes. **b**, hiPS-cell-derived podocytes and human immortalized podocytes stained for FcRn (magenta), a receptor for albumin and IgG transport. **c**, Confocal microscopy images of hiPS cells, hiPS-cell-derived podocytes and human immortalized podocytes exposed to exogenous albumin (HSA-FITC, green). Arrowheads indicate cells that exhibit albumin uptake. **d**, Quantification of HSA-FITC cells from **c**. Scale bars, 10 μm (**a**, bottom), 50 μm (**a**, top; **c**) and 100 μm (**b**). Data are mean \pm s.d.; $n = 3$; *** $P < 0.0001$.

In the kidney glomerulus, podocytes are also capable of sequestering large molecules, such as albumin, that leak into the urinary space or accumulate at the GBM, and this is mediated by the putative neonatal Fc receptor (FcRn)^{42,43}. We found that both the hiPS-cell-derived podocytes and immortalized podocytes express FcRn (Fig. 3b); however, the hiPS-cell-derived podocytes had a much greater ability to take up exogenous albumin (Fig. 3c, d). This could potentially relate to the observation that the hiPS-cell-derived podocytes showed higher levels of FcRn staining on their membrane processes (Fig. 3b).

A microfluidic organ-on-a-chip model of glomerular function

As in all living organs, the glomerular functions of the kidney that contribute to organ physiology and renal disease progression are highly sensitive to multiple factors in the local tissue microenvironment. These factors include tissue–tissue interactions (for example, between the podocyte and vascular endothelium) and cell–ECM interactions (with the intervening GBM), as well as cyclic mechanical forces and shear stresses due to glomerular blood and urine flow^{3,43}. Because conventional tissue-culture methods fail to reproduce the structural and functional characteristics of the glomerulus⁴¹, system-level analysis of podocyte biology and kidney disease mechanisms largely rely on animal studies. However, outcomes from animal studies often fail to recapitulate human physiological responses⁴⁴. For these reasons, microfluidic organ-on-a-chip culture models have been developed that better mimic functional units of human organs with organ-level structure and microenvironment, including tissue–tissue (for example, epithelial–endothelial) interfaces, fluid flows and cyclic mechanical deformations observed in

the lung and intestine^{45–47}. A microfluidic human kidney proximal-tubule-on-a-chip has been created that recapitulates multiple functions of the living proximal tubule⁴⁸, but it has not been possible to develop a model of the human glomerulus due to the lack of functional human podocytes. We therefore examined whether the hiPS-cell-derived podocytes that had been matured using the methods described above could be used to engineer a functional *in vitro* model of the human glomerular capillary wall, and if so, whether we could use this human glomerulus-on-a-chip to analyse human podocyte function and its sensitivity to microenvironmental cues and nephrotoxic drugs *in vitro*.

We designed a multifunctional microfluidic device that recapitulates the structural, functional and mechanical properties of a three-dimensional cross-section of the human glomerular capillary wall (Fig. 4a) using a previously published organ-on-a-chip fabrication protocol⁴⁹. The microfluidic device is composed of a flexible poly(dimethylsiloxane) (PDMS) elastomer that contains two closely opposed, parallel microchannels (1 \times 1 mm and 1 \times 0.2 mm, top and bottom channels, respectively) separated by a laminin-511-coated, porous flexible PDMS membrane (50- μm thick and 7- μm diameter pores with 40- μm spacing). Our goal was to culture hiPS-cell-derived podocytes on the top of the laminin-coated membrane and primary human glomerular endothelial cells on the opposite side of the same membrane to recapitulate the podocyte–GBM–endothelial interface, and to mimic the urinary and capillary compartments of the glomerulus, respectively (Fig. 4b). To model the dynamic mechanical strain observed in living glomeruli due to the cyclic pulsations of renal blood flow⁴³, we also incorporated two hollow chambers on either side of the central microfluidic channels

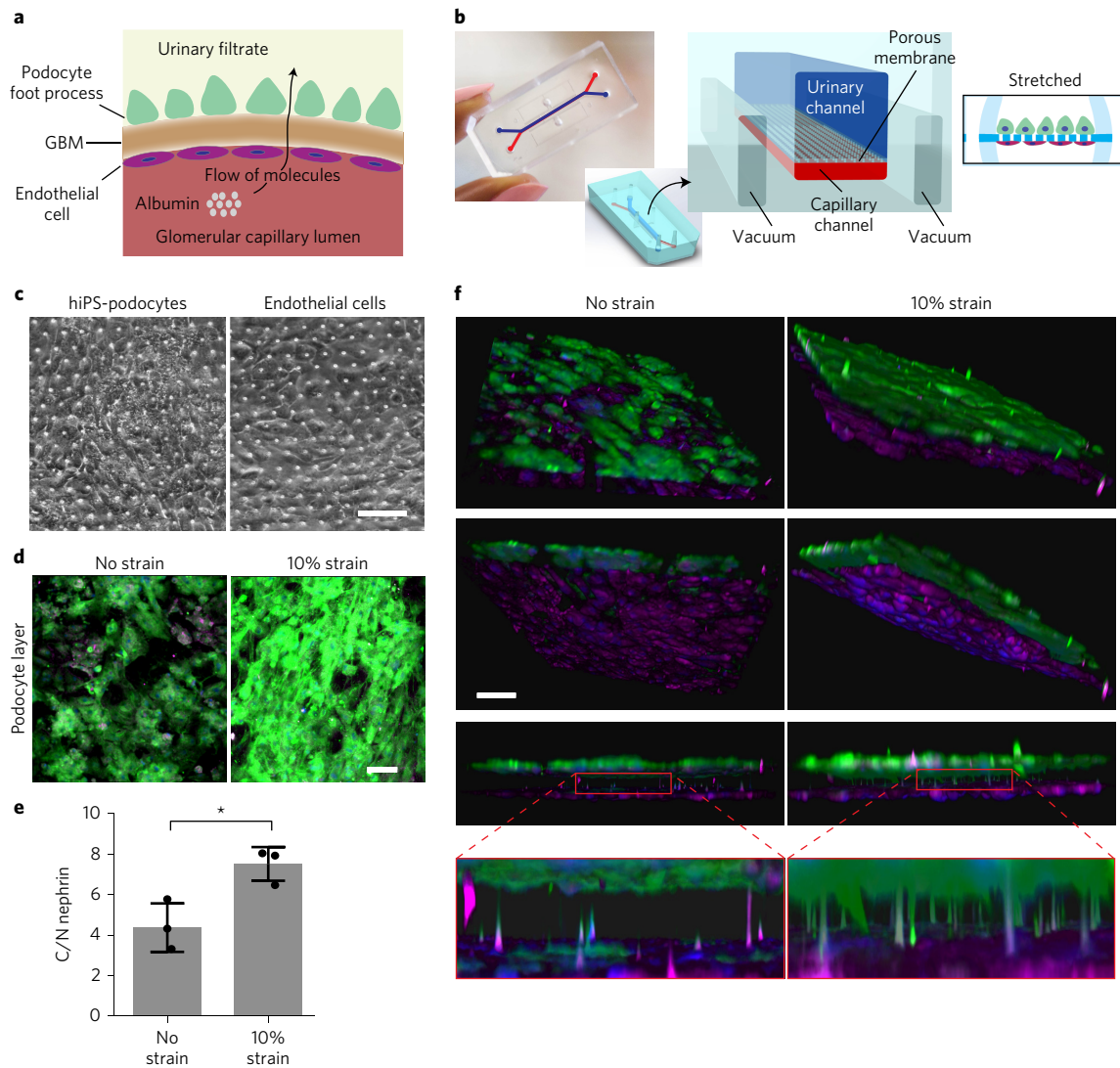


Figure 4 | Modelling the human glomerular capillary wall with an organ-on-a-chip microfluidic device. **a**, Schematic representation of glomerular capillary wall with podocytes and endothelial cells separated by the GBM. Arrow shows directional flow of molecules from the capillary lumen to urinary space. **b**, Photograph (left) and schematic (right) of a microfluidic organ-on-a-chip device with microchannels replicating the urinary and capillary compartments of the glomerulus. The GBM is replicated using a porous and flexible PDMS membrane functionalized with the ECM-protein laminin. Cyclic mechanical strain was applied to cell layers by stretching the flexible PDMS membrane using vacuum. **c**, Bright-field images of hiPS-cell-derived podocytes (left) differentiated in the organ-on-a-chip microdevice, and primary human glomerular endothelial cells (right) cultured on the opposite side of the flexible membrane. **d**, Immunofluorescence microscopy images of hiPS-cell-derived podocytes differentiated in the organ-on-a-chip microfluidic device with human glomerular endothelial cells (not shown) cultured on the opposite side of the PDMS membrane. Cells were differentiated under fluid flow only (no strain) or fluid flow and 10% mechanical strain (10% strain). Cells were stained for nephrin (green) and counterstained with DAPI (blue). **e**, Ratio of cytoplasmic to nuclear (C/N) nephrin in hiPS-cell-derived podocytes that were differentiated on-chip with or without mechanical strain. **f**, Three-dimensional reconstructed views of the tissue-tissue interface formed by hiPS-cell-derived podocytes (top, green) and human glomerular endothelial cells (bottom, magenta) showing that cyclic application of 10% strain enhanced the extension of podocyte cell processes through the pores of the flexible ECM-coated PDMS membrane so that they insert into the abluminal surface of the underlying glomerular endothelium (insets). Scale bars, 100 μm . Data are mean \pm s.d.; $n = 3$ (e); * $P < 0.05$.

(Fig. 4b), and applied cyclic suction (1 Hz, -85 kPa) to produce cyclic stretching (10% strain) and relaxation of the laminin-coated, flexible membrane and adherent cell layers, as was done previously in other mechanically active organs-on-chips⁴⁵.

To form a layer of differentiated podocytes, we seeded the hiPS-cell-derived intermediate mesoderm cells in the top channel of the device and differentiated them *in situ* using the podocyte-inducing differentiation medium in the presence or absence of fluid flow, or with a combination of fluid flow and cyclic mechanical strain to mimic physiological conditions. Notably, cells that were differentiated under fluid flow, or under a combination of flow and

mechanical strain, spread to a greater degree and showed higher levels of expression of cytoplasmic nephrin compared to cells in static control cultures (Supplementary Fig. 8a). Application of cyclic mechanical strain also significantly increased the levels of nephrin expression in the differentiated hiPS-cell-derived podocytes whether cultured alone ($P < 0.05$) or in the presence ($P < 0.0001$) of glomerular endothelial cells (Supplementary Fig. 8b), suggesting that mechanical forces can influence podocyte differentiation by enhancing expression of lineage-specific markers. In addition, these cells remained viable during culture in the microfluidic devices for at least two weeks of propagation, as measured by maintenance of

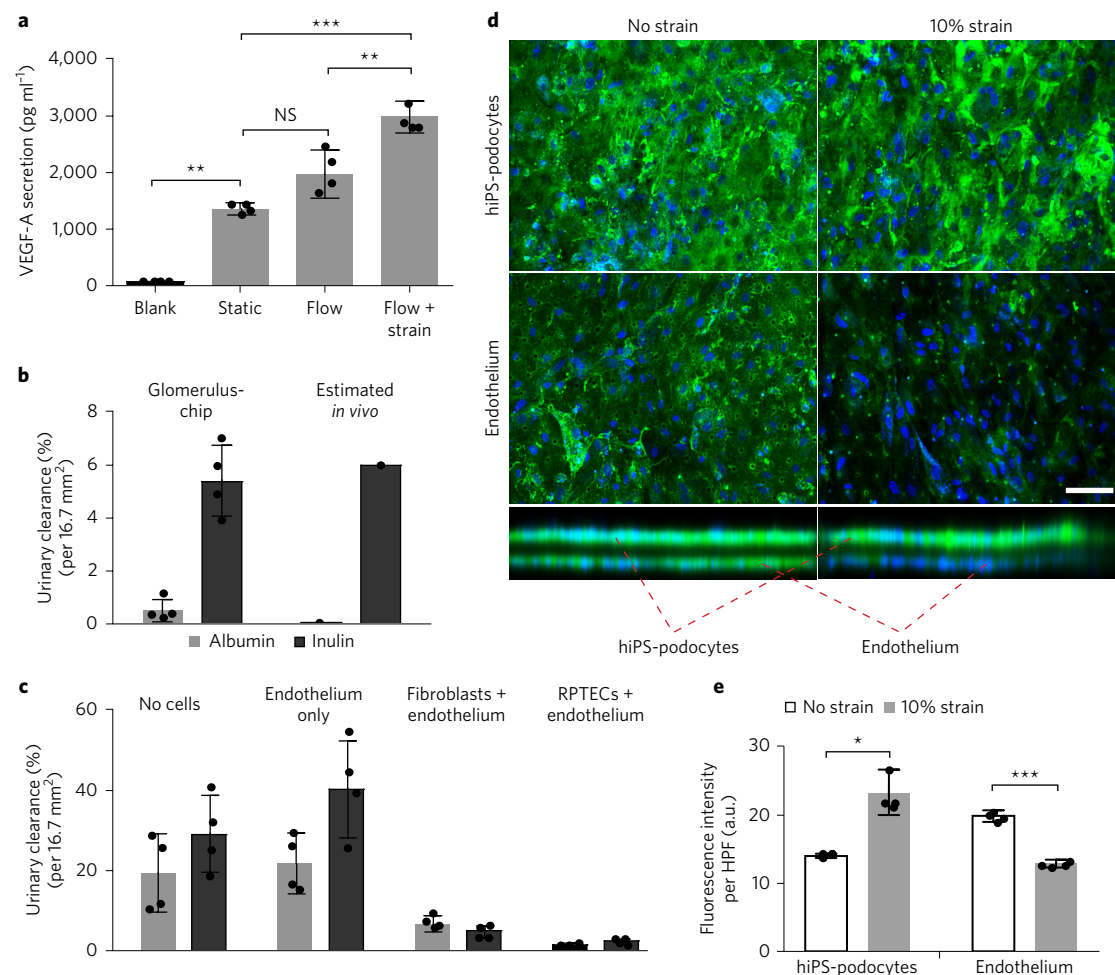


Figure 5 | Microfluidic organ-on-a-chip device reconstitutes kidney glomerular capillary function *in vitro*. **a**, Secretion of VEGF-A by hiPS-cell-derived podocytes differentiated in the microfluidic glomerulus-on-a-chip. Blank, no cells. **b**, Quantification of the glomerular filtration (urinary clearance) of albumin and inulin molecules that were continuously infused over 6 h into the capillary channel of the glomerulus chip that was lined by hiPS-cell-derived podocytes and human glomerular endothelial cells. Results are compared to *in vivo* values estimated based on the surface area of glomerular capillaries *in vivo*. **c**, Filtration of albumin and inulin in control microfluidic chips without human kidney podocytes quantified over 6 h of continuous infusion using the methods described above. RPTECs, renal proximal tubular epithelial cells. **d**, Immunofluorescence microscopy images showing the production and distribution of the basement membrane protein collagen type IV (green) in the microfluidic glomerulus chip in the presence or absence of physiological cyclic mechanical strain (bottom, side view of the glomerulus chip; nuclei were counterstained with DAPI in blue). **e**, Quantification of collagen type IV production by podocyte and endothelium layers in the glomerulus chip with or without mechanical strain as in **d**. a.u., arbitrary units. Scale bar, 100 μ m. Data are mean \pm s.d. (**a–c**, **e**); $n = 4$; * $P < 0.05$; ** $P < 0.001$; *** $P < 0.0001$; NS, not significant.

low levels of lactate dehydrogenase (LDH) release (Supplementary Fig. 9). These results demonstrate the feasibility of directing the differentiation of hiPS-cell-derived cells into glomerular podocytes on a chip (that is, when differentiated in the microfluidic devices) and that they remain viable for extended times in culture, which could enable the application of this organ-on-a-chip approach for patient-specific analyses in the future.

We recreated the tissue–tissue interface of the human glomerular capillary wall on-chip by seeding primary glomerular endothelial cells in the lower channel, and inducing differentiation of the hiPS-cell-derived podocytes in the top channel. Podocyte-inducing differentiation medium was perfused through the upper channel of the microfluidic chips lined by hiPS-cell-derived podocytes, whereas standard endothelial culture medium was perfused through the lower vascular channel lined by glomerular endothelial cells (Fig. 4c). After eight days of culture in the microfluidic device, we found that hiPS-cell-derived podocytes differentiated in the presence of both fluidic shear stress (0.0007 and 0.017 dyn cm⁻² in the top and bottom channels, respectively) and 10% cyclic strain

(1 Hz), exhibited a significant ($P < 0.0001$) increase in the intensity of cellular nephrin staining (Fig. 4d and Supplementary Fig. 8b) and a higher ratio of cytoplasmic to nuclear ($P < 0.05$) nephrin staining (Fig. 4e) compared to hiPS-cell-derived podocytes differentiated under fluid flow alone, again indicating a higher level of podocyte maturation.

Remarkably, confocal immunofluorescence microscopy analysis revealed that while the hiPS-cell-derived podocytes and glomerular endothelial cells remained in their respective channels on the opposite surfaces of the laminin-coated membrane when cultured under fluid flow alone, cyclic stretching of the tissue–tissue interface combined with fluid flow resulted in a significant increase in the number of podocyte cell processes that extended through the pores in the membrane to form contacts with the laminin-coated basal (abluminal) surface of the endothelium (Fig. 4f, Supplementary Fig. 10 and Supplementary Videos 1, 2), similar to those observed in intact glomerular tissues *in vivo*³. We also found that the hiPS-cell-derived podocytes differentiated in the microfluidic devices secrete VEGF-A (Fig. 5a). Notably, hiPS-cell-derived podocytes

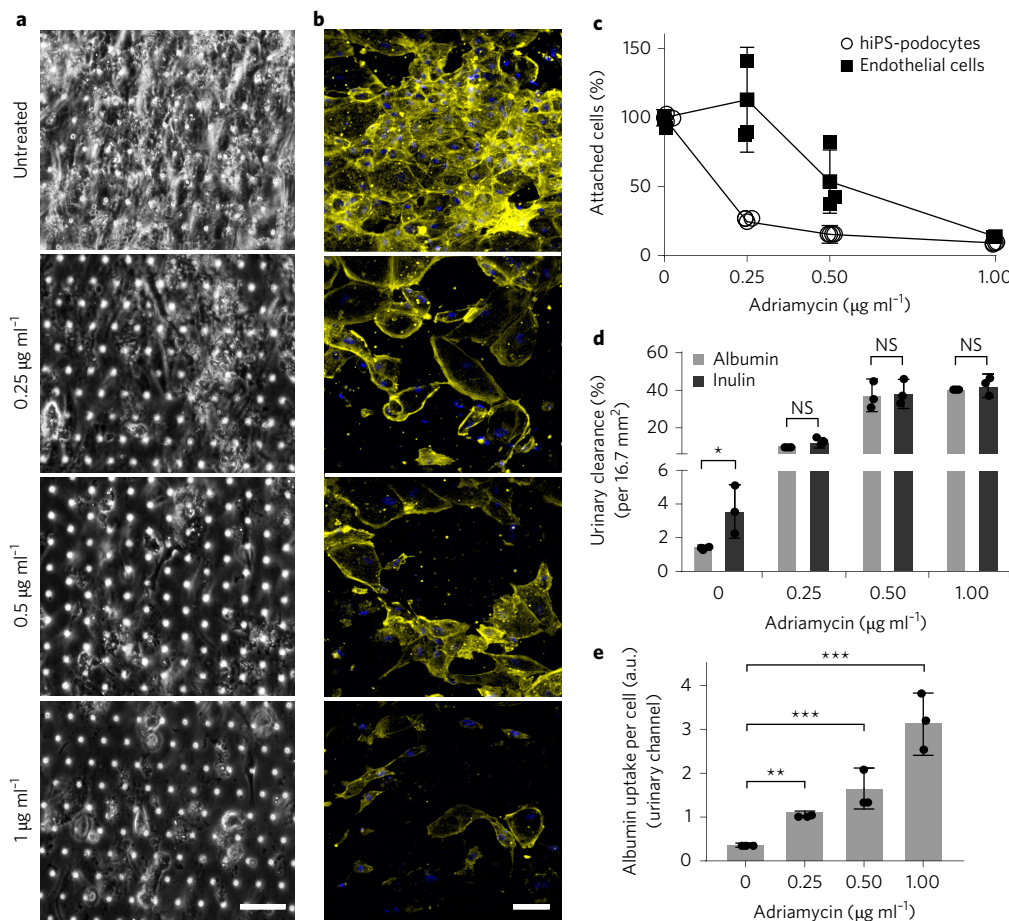


Figure 6 | Human glomerulus-on-a-chip mimics adriamycin-induced kidney glomerular injury. **a**, Phase-contrast images of the hiPS-cell-derived podocyte layer within the glomerulus chip continuously infused for five days with different concentrations of adriamycin through the underlying vascular channel lined by glomerular endothelial cells. **b**, Immunofluorescence microscopy images of the podocyte and endothelial cell layers within control and adriamycin-treated glomerulus chips stained with phalloidin (yellow) and counterstained with DAPI (blue). **c**, Dose-dependent effects of adriamycin exposure on cell adhesion within the podocyte and endothelial cell populations in the glomerulus chip measured after five days of drug treatment using quantification of DAPI-stained cells. **d**, Quantification of the dose-dependent effects of adriamycin exposure on glomerular filtration (urinary clearance in 6 h) of albumin and inulin in the glomerulus chip. **e**, Quantification of uptake of exogenous albumin in the urinary channel by the hiPS-cell-derived podocyte layer after adriamycin-induced injury. Scale bars, 100 μm . Data are mean \pm s.d. (**c–e**); $n = 3$; $*P < 0.05$; $**P < 0.001$; $***P < 0.0001$; NS, not significant.

cultured under physiological mechanical strain similar to that observed within living kidney⁴³ showed a significant increase in the levels of secreted VEGF-A relative to those propagated under static or fluid flow only. As VEGF-A secreted by podocytes is known to be required for vascular patterning and development of glomeruli *in vivo*⁵⁰, physiological cyclic deformations may contribute to control of this response in the forming embryonic kidney as well, and this organ-on-a-chip model could facilitate future investigations to address this hypothesis. Taken together, these results indicate that co-culture of hiPS-cell-derived podocytes and human kidney glomerular endothelial cells in the microfluidic device under physiological fluid flow and cyclic mechanical strain enable formation of organ-level structures that closely resemble the normal tissue–tissue interface of the glomerular capillary wall, which has previously not been possible to recapitulate using conventional cell-culture models. Given our ability to mimic a living portion of the human glomerulus on-chip, we then explored whether this microfluidic device could also reconstitute key kidney functions, such as the glomerular filtration barrier, which restricts permeability to large molecules (for example, albumin), but freely filters exogenous small molecules, such as inulin, from plasma⁵¹. Because cyclic mechanical deformation of the glomerulus occurs with every cardiac cycle^{2,43}, we performed these filtration studies while applying cyclic strain

(10% at 1 Hz) to the microfluidic human glomerulus-on-a-chip. We found that more than 99% of albumin was retained in the capillary channel even after 6 h of continuous perfusion through the microvascular channel of the human glomerulus-on-a-chip, whereas approximately 5% of inulin (out of a predicted maximal efficiency of 6% based on the surface area of the porous membrane relative to that of glomerular capillaries *in vivo*)⁵² was filtered into the urinary channel (Fig. 5b), which cannot be explained based on differences in diffusion coefficients alone.

More importantly, we did not obtain this differential in clearance between inulin and albumin when we co-cultured fibroblasts or renal proximal tubular epithelium with glomerular endothelium (that is, instead of podocytes), or when we used chips lined with glomerular endothelium alone or ECM-coated chips without any adherent cells (Fig. 5c and Supplementary Fig. 11). We also observed that chips lined only by hiPS-cell-derived podocytes that do not form a tight monolayer (Fig. 6b, control) only exhibit moderate selectivity to molecular filtration of albumin and inulin (not shown). Therefore, the human glomerulus-on-a-chip created by co-culturing the hiPS-cell-derived podocytes and primary human glomerular endothelial cells specifically mimics the normal filtration barrier of a functional glomerulus *in vitro*, at least for differential clearance of albumin and inulin.

During kidney development, there is a substantial increase in GBM synthesis and both podocytes and glomerular endothelial cells contribute to the GBM composition⁵³. Collagen type IV is a major component of the GBM and although it is produced by both podocytes and endothelial cells during early stages of glomerulogenesis, collagen type IV is predominately produced by glomerular podocytes in the fully mature GBM^{54,55}. Therefore, the molecular composition of the GBM and contributions from the different cell types correlate with the developmental status of the kidney glomerulus. We therefore examined whether the hiPS-cell-derived podocytes and glomerular endothelial cells cultured in the microfluidic organ-on-a-chip produce collagen type IV. These studies revealed that although collagen type IV is deposited by both cell types lining the microfluidic devices (Fig. 5d), collagen type IV was predominantly produced by the hiPS-cell-derived podocytes in microfluidic chips cultured under physiologically relevant mechanical strain (Fig. 5d,e) that also exhibit *in vivo*-like molecular clearance properties of glomerular capillaries (Fig. 5b). These results further underscore the importance of mechanical cues in kidney glomerular development and suggest a potential role in control of kidney-cell-specific responses. These findings also suggest that physiological mechanical strain is key requirement for the establishment of an organ-on-a-chip that mimics the molecular characteristics of a mature kidney glomerulus.

***In vitro* modelling of glomerular toxicity and proteinuria**

Given the limited availability of *in vitro* models that can closely mimic human kidney glomerular function and disease states, we explored if the microfluidic glomerulus chip lined with the hiPS-cell-derived podocytes and glomerular endothelial cells could model a kidney injury state. To test this, we exposed the glomerulus chips to the cancer drug adriamycin⁵⁶ (also known as doxorubicin) under continuous infusion through the endothelium-lined vascular channel, as it is administered intravenously in patients. Microscopy imaging revealed dose-dependent disruption of the podocyte layer and cell detachment in the urinary channel (Fig. 6a). Quantification of phalloidin-stained cells confirmed pronounced dose-dependent delamination of adriamycin-treated podocytes from the flexible ECM-coated membrane separating the urinary and vascular channels (Fig. 6b, c), and this correlated with decreasing cell viability as determined using a CCK-8 cytotoxicity assay (Supplementary Fig. 12a). Notably, significant podocyte delamination was observed at the clinically relevant concentration of 0.5 $\mu\text{g ml}^{-1}$ as well as at a lower dose (0.25 $\mu\text{g ml}^{-1}$) (Fig. 6b, c), and the remaining adherent podocytes exhibited retraction of their normally elongated cell processes (Supplementary Fig. 12b). Consistent with this observation, microfluidic chips treated with adriamycin exhibited significant loss of albumin from the vascular channel and increased entry into the urinary compartment (Fig. 6d), as is observed during adriamycin-induced podocyte injury *in vivo*⁵⁷. Additionally, the non-selective leakage of albumin through the glomerular filtration barrier induced by treatment with adriamycin resulted in increased uptake of albumin by the hiPS-cell-derived podocytes lining the urinary compartment of the microfluidic device (Fig. 6e). Together, these results show that the microfluidic human glomerulus-chip developed in this study mimics the development, function and disease manifestations of the kidney glomerular capillary wall.

Discussion

Organ-on-a-chip technology is not designed to engineer a whole living organ with all of its functionalities; instead, it is a synthetic biology approach that attempts to reconstitute essential functions of major functional units of organs that cannot be modelled currently using cell cultures or animal models. The challenge in this field is to recapitulate *in vivo* physiology of at least

a subset of functions that have value to research, clinical or drug-development communities, and then to progressively add additional functions over time. Therefore, we do not claim to have rebuilt a complete glomerulus in this study; however, we have reconstituted some of the critical functions of the human glomerular capillary wall that have, to our knowledge, not been modelled previously *in vitro*, and that may greatly advance research and drug development in this field. For example, our data demonstrate that this microfluidic model recapitulates the ability of the glomerular capillary to retain large proteins, such as albumin, in the circulation while excreting smaller molecules, which is one of the primary functions of the kidney glomerulus. We were also able to model drug toxicity that leads to albuminuria. This has not been possible using conventional cell-culture models that are currently used to study kidney biology, because these models lack an endothelium-lined vascular circuit and flow. Thus, the microfluidic organ-on-a-chip platform could potentially facilitate future investigations into the molecular mechanisms of glomerular filtration in the normal and diseased states.

Development of *in vitro* models of human glomerular function and regenerative medicine approaches for kidney diseases have been hindered in the past by the lack of availability of highly functional, differentiated human podocytes. Previous attempts to direct human pluripotent stem-cell differentiation into kidney cells through embryoid bodies and organoids have been limited by high levels of heterogeneity and production of podocytes-like cells with a predominantly immature phenotype. Therefore, it has remained unclear which signals within the stem-cell microenvironment specifically drive podocyte lineage commitment from an undifferentiated state. By contrast, the induction protocol we describe here provides a highly efficient (over 90%) method for the directed differentiation of hiPS cells into kidney podocytes, and we show that these cells exhibit morphological, molecular and functional characteristics of mature human podocytes. The high (more than 90%) efficiency of this method for inducing formation of mature tissue-specific epithelial cells from hiPS cell lines may be based on our use of organ-specific ECM (laminin) in addition to specific soluble signalling factors. In addition, we show that the partially specialized hiPS-cell-derived intermediate mesoderm cells can be cultured in microfluidic devices and induced to differentiate into mature podocytes with high efficiency on-chip. Moreover, by leveraging these results, we engineered an *in vitro* model of the human glomerular capillary wall that permits the application of physiological fluid flow and cyclic strain to two opposing cell layers of the human glomerular capillary wall separated by a porous, ECM-coated flexible membrane, while simultaneously enabling analysis of molecular filtration across the tissue barrier. These studies confirmed that the engineered human-glomerulus-on-a-chip recapitulates some of the normal molecular filtration properties of the functional human kidney glomerular capillary wall and replicates pharmacologically induced podocyte injury and albuminuria as seen in patients, a feature that cannot be replicated using traditional *in vitro* models or organoid cultures. We also found that application of physiologically relevant mechanical cues (for example, cyclic strain and flow) further augmented podocyte differentiation and maturation.

Outlook

Because existing immortalized podocyte cell lines and cultures poorly mimic glomerular function, and animal studies often fail to predict human physiological responses, our findings could provide a better *in vitro* system for predicting nephrotoxicity and therapeutic development. The glomerulus-on-a-chip might be particularly noteworthy for personalized medicine applications, for example, to study hereditary forms of nephrotic syndrome that often lead to more severe outcomes using iPSC cells that have been derived

from patients or modified by precision genome engineering, given that almost all mutated gene products have been shown to localize to podocytes⁵⁸. It is conceivable that the podocyte differentiation method, as well as the human glomerulus-on-a-chip described here, could also facilitate investigations to illuminate developmentally regulated events in kidney pathophysiology and provide a low-cost alternative to animal models for the development of preventative and therapeutic interventions for both genetic and acquired forms of human kidney disease. It would also be of interest to explore whether these hiPS-cell-derived podocytes might be useful for tissue engineering, 3D printing of organs and cell-based therapies for regenerative medicine in the future.

Methods

Cell culture. All cell lines were obtained under appropriate material transfer agreements and approved by all involved institutional review boards, and tested for mycoplasma contamination (using the MycoAlert Mycoplasma Detection kit from Lonza, LT07-318) before use. The hiPS cell lines PGP1 (the Personal Genome Project)⁵⁹, IMR-90-1 and IISH3i CB6 (WiCell Research Institute) were propagated on tissue-culture plates that were coated with Matrigel (BD Biosciences) by using mTeSR1 medium (Stem Cell Technologies). hiPS cells were incubated at 37 °C in 5% CO₂, and passaged every 5–7 days by treatment with StemPro accutase (Thermo Fisher Scientific). Conditionally immortalized human podocytes⁵⁴ (Mundel laboratory at Massachusetts General Hospital and Harvard Medical School) were propagated at the permissive temperature of 33 °C in 5% CO₂ by using complete medium with CultureBoost-R (Cell Systems), and passaged every 4–5 days by treatment with 0.05% trypsin-EDTA (GIBCO). For induction of the podocyte phenotype, the immortalized human podocytes were cultured at 37 °C in 5% CO₂ for 10–14 days. Human glomerular microvascular endothelial cells (Cell Systems) were cultured at 37 °C in 5% CO₂ by using complete medium with CultureBoost-R (Cell Systems), and passaged every 6–7 days by treatment with 0.05% trypsin-EDTA. Human glomerular microvascular endothelial cells at passage 6–8 were used for all experiments. PGP1 fibroblasts were also obtained from the Personal Genome Project and cultured according to the supplier's protocol. Primary human renal proximal tubule epithelial cells (ScienCell; catalogue number 4100 and TAN record 664) were cultured according to the supplier's instructions and used at passage 3 (15 population doublings) or less.

hiPS cell adhesion and propagation on ECM-coated surfaces. Tissue-culture-treated plates were incubated for 2 h at room temperature with 5 µg ml⁻¹ of collagen type I (BD Biosciences), laminin-511 (BioLamina), laminin-511-E8 (Iwai North America), or laminin-521 (BioLamina). hiPS cells were dissociated by treatment with enzyme-free cell dissociation buffer (GIBCO) and cultured on the ECM-coated surfaces at 4 × 10⁴ cells cm⁻² in serum-free DMEM/F12 (GIBCO) for 3 h. For prolonged culture, the cells were fed daily with mTeSR1 medium.

Differentiation of hiPS cells into podocytes. hiPS cells were first dissociated from Matrigel-coated plates by treatment with StemPro accutase (Thermo Fisher Scientific) and centrifuged twice at 1,200 r.p.m. for 5 min each in DMEM/F12. The cells were plated on laminin-511-E8-coated plates with a mesoderm differentiation medium consisting of DMEM/F12 with GlutaMax (GIBCO) supplemented with 100 ng ml⁻¹ activin A (Thermo Fisher Scientific), 3 µM CHIR99021 (Stemgent), 10 µM Y27632 (TOCRIS) and 1 × B27 serum-free supplement (GIBCO). After 2 days of differentiation, the cells were incubated for a minimum of 14 days with an intermediate mesoderm induction medium consisting of DMEM/F12 with GlutaMax supplemented with 100 ng ml⁻¹ BMP7 (Thermo Fisher Scientific), 3 µM CHIR99021 and 1 × B27 serum-free supplement. To induce the podocyte phenotype, the intermediate mesoderm cells were dissociated by treatment with 0.05% trypsin-EDTA and cultured at a 1:4 splitting density on freshly prepared laminin-511-E8-coated plates, and fed daily for 4–5 days with a podocyte induction medium consisting of DMEM/F12 with GlutaMax supplemented with 100 ng ml⁻¹ BMP7, 100 ng ml⁻¹ activin A, 50 ng ml⁻¹ VEGF (Thermo Fisher Scientific), 3 µM CHIR99021, 1 × B27 serum-free supplement, and 0.1 µM all-trans retinoic acid (Stem Cell Technologies).

Quantitative real-time PCR. RNA was purified using an RNeasy mini kit (Qiagen, Valencia, California, USA). qPCR was performed with the iScript cDNA synthesis kit (Bio-Rad, Hercules, California, USA) and iTaq Sybr Green Supermix (Bio-Rad) using a CFX96 real-time PCR machine (Bio-Rad). β-actin, GAPDH or cyclophilin controlled for cDNA content. Primers used for qPCR are described in Supplementary Table 1.

Flow cytometry. hiPS cells, hiPS-cell-derived podocytes and immortalized human podocytes were collected by treatment with 0.05% trypsin-EDTA, the trypsin was quenched with 10% fetal bovine serum in DMEM/F12, followed by fixation of the cells for 30 min at room temperature with 2% paraformaldehyde in PBS. Cells were permeabilized with saponin permeabilization buffer (0.1%

saponin and 0.1% bovine serum albumin (BSA) in PBS) for 30 min at room temperature and then incubated at room temperature for 1 h with the following antibodies, OCT4 conjugated to phycoerythrin (PE) (Stem Cell Technologies, 60093PE); WT1 conjugated to allophycocyanin (APC) (LifeSpan Biosciences, LS-C224662/57444); nephrin conjugated to PE-Cy5 (Bioss, bs-10233R-PE-Cy5); or a combination of nephrin-PE-Cy5 and WT1-APC. Cells were washed twice with saponin permeabilization buffer before analysis. Data were acquired with an LSRFortessa flow cytometer (BD Biosciences) and analysed with FlowJo software. The percentage of positive cells was determined by comparing experimental cells to undifferentiated hiPS cells and immortalized human podocytes.

Immunostaining and microscopy. All bright field images were captured using a Nikon EclipseTS100-F microscope equipped with a Zeiss AxioCam MRc 5. Cell size measurements were determined using ImageJ software. For immunostaining, cells were fixed with 4% paraformaldehyde in PBS for 30 min at room temperature and permeabilized with 0.125% triton X-100 in PBS for 5 min. Cells were then blocked by treatment with a solution of 2% BSA and 0.125% triton X-100 in PBS for 30 min at room temperature. The cells were incubated with primary antibodies in permeabilization buffer overnight at 4 °C, followed by incubation with secondary antibodies in permeabilization buffer for 1 h at room temperature. The cells were counterstained with 4',6-diamidino-2-phenylindole (DAPI, Invitrogen). The primary antibodies used included β1 integrin (Abcam, ab24693), OCT4 (R&D Systems, AF1759), TRA-1-60 (Abcam, ab16288), gooseoid (R&D Systems, AF4086), brachyury (Abcam, ab20680), HAND1 (Abcam, ab196622), PAX2 (Invitrogen, 71-6000), OSR1 (Novus Biologicals, H00130497-M04), WT1 (Millipore, MAB4234), nephrin (Progen, GP-N2), podocin (Abcam, ab50339), VE-cadherin (Santa Cruz Biotech, sc-9989), PKCλ/ι (Santa Cruz Biotech, sc-727), collagen type IV (Abcam, ab6586) and FcRn (Santa Cruz Biotech, sc-271745). Alexa Fluor 488- and Alexa Fluor 594-conjugated antibodies (Invitrogen) were used as secondary antibodies. Immunostained cells were visualized with a Zeiss Axio Observer Z1 microscope equipped with a Cool Snap HQ2 camera and Carl Zeiss Zen software, and images were processed in Adobe Photoshop CS5. Confocal images were acquired with a Leica SP5 X MP inverted microscope using a 25×/0.95 water objective. Confocal images, videos and co-localization measurements were performed with IMARIS software version 8.1. Quantification of hiPS-cell-derived podocyte cell processes at the podocyte-endothelial cell interface in the organ-on-chip microfluidic devices was also performed using IMARIS software such that the region of interest comprised nephrin-positive cellular protrusions within the middle 20 µm of the flexible PDMS membrane separating the podocyte and endothelial cell layers; threshold and particle analysis were performed using Fiji for ImageJ.

EdU-incorporation assay. Cell proliferation was analysed by using the Click-iT EdU imaging kit with Alexa Fluor 594 (Invitrogen) following the manufacturer's protocol. In brief, cells were incubated with 10 µM EdU solution in cell-culture medium for 24 h at 37 °C. The cells were fixed with 4% paraformaldehyde for 20 min at room temperature, followed by washing with 3% BSA in PBS, and then permeabilized by treatment with 0.5% triton X-100 for 20 min at room temperature. The cells were incubated with the Click-iT reaction cocktail for 30 min followed by antibody staining and DAPI counterstaining as described above. Samples were visualized using a Zeiss Axio Observer Z1 microscope equipped with a Cool Snap HQ2 camera and Carl Zeiss Zen software and images were processed in Adobe Photoshop CS5.

Western blot. Whole-cell extracts were lysed with RIPA buffer (50 mM Tris-HCl, 150 mM NaCl, 1% NP-40, 0.5% sodium deoxycholate and 0.1% SDS), fractionated by SDS-PAGE and transferred to a nitrocellulose membrane using a transfer apparatus according to the manufacturer's protocols (Bio-Rad). The membranes were blocked by treatment with 5% non-fat milk in TBST (50 mM Tris-HCl, 150 mM NaCl, 0.1% Tween-20), followed by incubation with rabbit anti-phospho-PKCι (pThr555)/PKCλ (pThr563) (Thermo Fisher Scientific, 44-968G), rabbit anti-PKCλ/ι antibody (Santa Cruz Biotech, sc-727), or mouse anti-GAPDH antibody (Millipore, MAB374). A horseradish-peroxidase-conjugated goat anti-rabbit or -mouse antibody was then added, and the membranes were developed with the ECL Plus system (GE Healthcare) according to the manufacturer's protocol. Quantification of the band intensity was performed using ImageJ software.

Scanning electron microscopy. Cells were differentiated on plastic coverslips (Thermo Fisher Scientific) or in the microfluidic organ-on-a-chip device by following protocols described above. Cells were fixed with 2.5% glutaraldehyde in 0.1 M sodium cacodylate buffer (Electron Microscopy Sciences) for 1 h followed by 1% osmium tetroxide in 0.1 M sodium cacodylate (Electron Microscopy Sciences) for 1 h and then dehydrated in ascending grades (30%, 50%, 70%, 80%, 90%, 95% and 100%) of ethanol. Samples were then chemically dried with hexamethyldisilazane (Electron Microscopy Sciences) in a desiccator overnight. Before imaging, samples were mounted and sputter-coated with a thin layer of gold (for coverslip samples) or 5-nm layer of platinum-palladium (for microfluidic devices) and imaged using a Zeiss Supra55VP field emission microscope with a secondary detector.

Albumin-uptake assay. Cells were incubated with 100 $\mu\text{g ml}^{-1}$ human serum albumin (HSA) conjugated to FITC (HSA-FITC) (Abcam) in basal DMEM/F12 medium for 1 h at 37 °C. For negative control, cells were incubated with HSA-FITC at 4 °C. The cells were fixed with 4% paraformaldehyde and then counterstained with DAPI. Samples were visualized with a Leica SP5 X MP inverted confocal microscope and the images were processed in ImageJ.

Fabrication of the microfluidic organ-on-a-chip device. Microfluidic organ-on-chip devices were produced by modification of a previously published protocol⁴⁵, starting from molds that were fabricated out of Prototherm 12120 using stereolithography (Proto Labs). The ‘urinary’ and ‘microvascular’ channels of the devices were cast from polydimethyl siloxane (PDMS) at a 10:1 w/w base to curing agent ratio (Ellsworth Adhesives). The prepolymer mixture was degassed and then cured for 4 h to overnight at 60 °C. The device contains two fluidic channels (a 1 × 1 mm urinary channel and 1 × 0.2 mm microvascular channel), two vacuum channels parallel to the fluidic channels and ports for all fluidic and vacuum channels. The urinary and microvascular channels are separated by a porous PDMS membrane, which was produced by casting against a DRIE-patterned silicon wafer (50 × 50 mm) consisting of 50- μm high and 7- μm diameter posts spaced 40 μm apart. To produce through-holes in the membrane using the microfabricated post array, we first poured 100 μl of PDMS onto the wafer and then compressed a polycarbonate backing against the post array, followed by baking at 60 °C for 4 h. The porous PDMS membrane was bonded to the top component of the device by using oxygen plasma treatment (40 W, 800 mbar, 40 s; Plasma Nano, Diener Electronic) followed by bonding of the top-membrane assembly to the bottom component containing the microvascular channel (1 mm wide × 0.2 mm high) and matching vacuum channels.

Cell culture and differentiation in the microfluidic organ-on-a-chip. Before cell culture, the microfluidic devices were activated/sterilized by treatment with oxygen plasma (100 W, 15 s.c.c.m., 30 s; PlasmaEtcher PE-00, Plasma Etch). The porous PDMS membranes that separate the two fluidic channels were incubated on both sides with 50 $\mu\text{g ml}^{-1}$ laminin-511 in PBS with calcium and magnesium overnight at 37 °C. Primary human glomerular endothelial cells (4×10^4 cells) were seeded in the bottom channel of the device by inversion for 3 h in complete medium with CultureBoost-R, followed by seeding of the top channel with 4×10^4 hiPS-cell-derived intermediate mesoderm cells for 3 h in the podocyte-inducing medium described above. The respective medium for each fluidic channel was refreshed daily and the microfluidic devices were incubated at 37 °C in 5% CO₂ under static conditions for 48 h. The attached cells were then continuously perfused with the respective cell-culture medium by using an Ismatec IPC-N digital peristaltic pump (Cole-Parmer) at a volumetric flow rate of 60 $\mu\text{l h}^{-1}$ (shear stress of 0.0007 dyn cm⁻² for the top channel and 0.017 dyn cm⁻² for the bottom channel), and cyclic stretching was continuously applied to the microfluidic devices as described below. The cell-lined microfluidic devices were cultured for a minimum of eight days before analyses and drug toxicity studies. The levels of cell-secreted VEGF-A was examined using the human VEGF-A ELISA kit from RayBiotech per the manufacturer’s protocol.

Microfluidic glomerulus chips lined with hiPS-cell-derived podocytes and glomerular endothelial cells cultured under fluid flow and mechanical strain were used for all drug toxicity studies. Adriamycin (D-4000, LC Laboratories) was used at the indicated concentrations in serum-free medium (SF-4Z0-500-R, Cell Systems) and continuously infused through the vascular channel of the microfluidic chips for up to five days of microfluidic culture.

Mechanical actuation of the microfluidic organ-on-a-chip. Microfluidic cell cultures were mechanically actuated by using a programmable vacuum regulator system built in-house. The system consists of a vacuum regulator (ITV0091-2BL, SMC Corporation of America) that was electronically controlled by an Arduino Leonardo and MAX517 digital to analogue converter. The regulator outputs a sinusoidal vacuum profile with a user-settable amplitude and frequency. Cyclic strain (around 10%) was applied to microfluidic organs-on-chips at an amplitude of –85 kPa and frequency of 1 Hz.

Inulin and albumin filtration assay. Urinary clearance of inulin and albumin was evaluated by using cell-lined microfluidic devices subjected to both fluid flow and cyclic strain, and cultured for a minimum of eight days. For filtration studies, both the top and bottom channels of the device were perfused with complete medium with CultureBoost-R. Cell-culture medium supplemented with a mixture of 10 $\mu\text{g ml}^{-1}$ inulin conjugated to FITC (Sigma-Aldrich) and 100 $\mu\text{g ml}^{-1}$ albumin conjugated to Alexa Fluor 555 (ThermoFisher Scientific) was continuously perfused through the microvascular channel for 6 h while applying cyclic strain. The fluorescence intensity of the outflow from each channel was measured by using a Synergy NEO HTS Multi-Mode microplate reader (BioTek). The amount of inulin or albumin filtered from the microvascular to the urinary channel was calculated by using the equation for renal clearance:

$$\text{Urinary clearance} = ([U] \times UV) / [P]$$

Where [U] = urinary concentration, UV = urinary volume, and [P] = plasma or microvascular concentration. The per cent urinary clearance was calculated from a ratio of urinary clearance to urinary volume.

Cell-viability assay. Cell viability was examined by measurement of released LDH from microfluidic device medium outflow, spent medium from cells cultured on tissue-culture plates, cell lysate (positive control) or fresh cell-culture medium (negative control) by using the CytoTox 96 NonRadioactive Cytotoxicity Assay kit (Promega) per the manufacturer’s protocol. Absorbance was measured with a Synergy NEO HTS Multi-Mode microplate reader (BioTek).

Data availability. All data supporting the finding of this study are included within the paper and its Supplementary Information.

Received 1 September 2016; accepted 29 March 2017; published 10 May 2017

References

- Kardasz, S. The function of the nephron and the formation of urine. *Anaesth. Intensive Care Med.* **10**, 265–270 (2009).
- Greka, A. & Mundel, P. Cell biology and pathology of podocytes. *Annu. Rev. Physiol.* **74**, 299–323 (2012).
- Reiser, J. & Sever, S. Podocyte biology and pathogenesis of kidney disease. *Annu. Rev. Med.* **64**, 357–366 (2013).
- Benam, K. H. *et al.* Engineered *in vitro* disease models. *Annu. Rev. Pathol.* **10**, 195–262 (2015).
- Thomson, J. *et al.* Embryonic stem cell lines derived from human blastocysts. *Science* **282**, 1145–1147 (1998).
- Takahashi, K. *et al.* Induction of pluripotent stem cells from adult human fibroblasts by defined factors. *Cell* **131**, 861–872 (2007).
- Song, B. *et al.* The directed differentiation of human iPS cells into kidney podocytes. *PLoS ONE* **7**, e46453 (2012).
- Sharmin, S. *et al.* Human induced pluripotent stem cell-derived podocytes mature into vascularized glomeruli upon experimental transplantation. *J. Am. Soc. Nephrol.* **27**, 1778–1791 (2016).
- Ciampi, O. *et al.* Generation of functional podocytes from human induced pluripotent stem cells. *Stem Cell. Res.* **17**, 130–139 (2016).
- Takasato, M. *et al.* Kidney organoids from human iPS cells contain multiple lineages and model human nephrogenesis. *Nature* **526**, 564–568 (2015).
- Morizane, R. *et al.* Nephron organoids derived from human pluripotent stem cells model kidney development and injury. *Nat. Biotechnol.* **33**, 1193–1200 (2015).
- Jones, D. L. & Wagers, A. J. No place like home: anatomy and function of the stem cell niche. *Nat. Rev. Mol. Cell Biol.* **9**, 11–21 (2008).
- Ingber, D. E., Wang, N. & Stamenovic, D. Tensegrity, cellular biophysics, and the mechanics of living systems. *Rep. Prog. Phys.* **77**, 046603 (2014).
- Watanabe, K. *et al.* A ROCK inhibitor permits survival of dissociated human embryonic stem cells. *Nat. Biotechnol.* **25**, 681–686 (2007).
- Mummery, C. *et al.* Differentiation of human embryonic stem cells and induced pluripotent stem cells to cardiomyocytes: a methods overview. *Circ. Res.* **111**, 344–358 (2012).
- Musah, S. *et al.* glycosaminoglycan-binding hydrogels enable mechanical control of human pluripotent stem cell self-renewal. *ACS Nano* **6**, 10168–10177 (2012).
- Musah, S. *et al.* Substratum-induced differentiation of human pluripotent stem cells reveals the coactivator YAP is a potent regulator of neuronal specification. *Proc. Natl Acad. Sci. USA* **111**, 13805–13810 (2014).
- Li, D. *et al.* Role of mechanical factors in fate decisions of stem cells. *Regen. Med.* **6**, 229–240 (2011).
- Rodin, S. *et al.* Long-term self-renewal of human pluripotent stem cells on human recombinant laminin-511. *Nat. Biotechnol.* **28**, 611–615 (2010).
- Patey, N., Halbwachs-Mecarelli, L., Droz, D., Lesavre, P. & Noel, L. H. Distribution of integrin subunits in normal human kidney. *Cell Adhes. Commun.* **2**, 159–167 (1994).
- Pavenstädt, H., Kriz, W. & Kretzler, M. Cell biology of the glomerular podocyte. *Physiol. Rev.* **83**, 253–307 (2003).
- Miner, J. Renal basement membrane components. *Kidney Int.* **56**, 2016–2024 (1999).
- Kanasaki, K. *et al.* Integrin β 1-mediated matrix assembly and signaling are critical for the normal development and function of the kidney glomerulus. *Dev. Biol.* **313**, 584–593 (2008).
- Pozzi, A. *et al.* β 1 integrin expression by podocytes is required to maintain glomerular structural integrity. *Dev. Biol.* **316**, 288–301 (2008).
- Pietilä, I. & Vainio, S. J. Kidney development: an overview. *Nephron Exp. Nephrol.* **126**, 40–44 (2014).
- Mae, S.-I. *et al.* Monitoring and robust induction of nephrogenic intermediate mesoderm from human pluripotent stem cells. *Nat. Commun.* **4**, 1367 (2013).
- Taguchi, A. & Nishinakamura, R. Nephron reconstitution from pluripotent stem cells. *Kidney Int.* **87**, 894–900 (2015).

28. Kitamoto, Y., Tokunaga, H., Miyamoto K. & Tomita, K. VEGF is an essential molecule for glomerular structuring. *Nephrol. Dial. Transplant.* **17** (Suppl. 9), 25–27 (2002).
29. Gerber H. P. *et al.* VEGF is required for growth and survival in neonatal mice. *Development* **126**, 1149–1159 (1999).
30. Zhong, Y. *et al.* Novel retinoic acid receptor alpha agonists for treatment of kidney disease. *PLoS ONE* **6**, e27945 (2011).
31. Taguchi, A. *et al.* Redefining the *in vivo* origin of metanephric nephron progenitors enables generation of complex kidney structures from pluripotent stem cells. *Cell Stem Cell* **14**, 53–67 (2014).
32. Davies, J. A. Morphogenesis of the metanephric kidney. *ScientificWorldJournal* **2**, 1937–1950 (2002).
33. Brennan, H. C., Nijjar, S. & Jones, E. A. The specification and growth factor inducibility of the pronephric glomus in *Xenopus laevis*. *Development* **126**, 5847–5856 (1999).
34. Saleem, M. *et al.* A conditionally immortalized human podocyte cell line demonstrating nephrin and podocin expression. *J. Am. Soc. Nephrol.* **13**, 630–638 (2002).
35. Tabar, V. & Studer, L. Pluripotent stem cells in regenerative medicine: challenges and recent progress. *Nat. Rev. Genet.* **15**, 82–92 (2014).
36. Quaggin, S. Transcriptional regulation of podocyte specification and differentiation. *Microsc. Res. Tech.* **57**, 208–211 (2002).
37. Floege, J. *et al.* Visceral glomerular epithelial cells can proliferate *in vivo* and synthesize platelet-derived growth factor B-chain. *Am. J. Pathol.* **142**, 637–650 (1993).
38. Kestilä, M. *et al.* Positionally cloned gene for a novel glomerular protein—nephrin—is mutated in congenital nephrotic syndrome. *Mol. Cell* **1**, 575–582 (1998).
39. Ruotsalainen, V. *et al.* Nephrin is specifically located at the slit diaphragm of glomerular podocytes. *Proc. Natl Acad. Sci. USA* **96**, 7962–7967 (1999).
40. Satoh, D. *et al.* aPKC λ maintains the integrity of the glomerular slit diaphragm through trafficking of nephrin to the cell surface. *J. Biochem.* **156**, 115–128 (2014).
41. Shankland, S. J., Pippin, J. W., Reiser J. & Mundel, P. Podocytes in culture: past, present, and future. *Kidney Int.* **72**, 26–36 (2007).
42. Saleem, M. A. One hundred ways to kill a podocyte. *Nephrol. Dial. Transplant.* **30**, 1266–1272 (2015).
43. Peti-Peterdi, J., Kidokoro, K. & Riquier-Brisson, A. Novel *in vivo* techniques to visualize kidney anatomy and function. *Kidney Int.* **88**, 44–51 (2015).
44. Greek, R. & Menache, A. Systematic reviews of animal models: methodology versus epistemology. *Int. J. Med. Sci.* **10**, 206–221 (2013).
45. Huh, D. *et al.* Reconstituting organ-level lung functions on a chip. *Science* **328**, 1662–1668 (2010).
46. Kim, H. J., Li, H., Collins, J. J. & Ingber, D. E. Contributions of microbiome and mechanical deformation to intestinal bacterial overgrowth and inflammation in a human gut-on-a-chip. *Proc. Natl Acad. Sci. USA* **113**, E7–E15 (2016).
47. Bhatia, S. N. & Ingber, D. E. Microfluidic organs-on-chips. *Nat. Biotechnol.* **32**, 760–772 (2014).
48. Jang, K.-J. *et al.* Human kidney proximal tubule-on-a-chip for drug transport and nephrotoxicity assessment. *Integr. Biol.* **5**, 1119–1129 (2013).
49. Huh, D. *et al.* Microfabrication of human organs-on-chips. *Nat. Protoc.* **8**, 2135–2157 (2013).
50. Eremina, V. & Quaggin, S. E. The role of VEGF-A in glomerular development and function. *Curr. Opin. Nephrol. Hypertens.* **13**, 9–15 (2004).
51. Tojo, A. & Kinugasa, S. Mechanisms of glomerular albumin filtration and tubular reabsorption. *Int. J. Nephrol.* **2012**, 481520 (2012).
52. Bohle, A. *et al.* Human glomerular structure under normal conditions and in isolated glomerular disease. *Kidney Int. Suppl.* **54** (Suppl. 67), S186–S188 (1998).
53. Abrahamson, D. R. Role of the podocyte (and glomerular endothelium) in building the GBM. *Semin. Nephrol.* **32**, 342–349 (2012).
54. Miner, J. H. Organogenesis of the kidney glomerulus: focus on the glomerular basement membrane. *Organogenesis* **7**, 75–82 (2011).
55. Abrahamson, D. R., Hudson, B. G., Stroganova, L., Borza, D.-B. & St John, P. L. Cellular origins of type IV collagen networks in developing glomeruli. *J. Am. Soc. Nephrol.* **20**, 1471–1479 (2009).
56. Zhang, H.-T. T. *et al.* The mTORC2/Akt/NF κ B pathway-mediated activation of TRPC6 participates in adriamycin-induced podocyte apoptosis. *Cell. Physiol. Biochem.* **40**, 1079–1093 (2016).
57. Zhong, F., Wang, W., Lee, K., He, J. C. & Chen, N. Role of C/EBP α in adriamycin-induced podocyte injury. *Sci. Rep.* **6**, 33520 (2016).
58. Friedman, D. J. & Pollak, M. R. Genetics of kidney failure and the evolving story of APOL1. *J. Clin. Invest.* **121**, 3367–3374 (2011).
59. Ball, M. P. *et al.* A public resource facilitating clinical use of genomes. *Proc. Natl Acad. Sci. USA* **109**, 11920–11927 (2012).

Acknowledgements

This work was supported by the Defense Advanced Research Projects Agency under Cooperative Agreement Number W911NF-12-2-0036 and the Wyss Institute for Biologically Inspired Engineering at Harvard University. S.M. was supported by a Dean's Postdoctoral Fellowship from Harvard Medical School, a UNCF-Merck Postdoctoral Fellowship, a Postdoctoral Enrichment Program Award from the Burroughs Wellcome Fund and an NIH/NIDDK Nephrology Training Grant (4T32DK007199-39). We thank the Wyss Institute Microfabrication team for organ-chip production; A. P. Mehr, K. Jang, A. Bahinski and R. Prantil-Baun for helpful discussions; E. Jiang, Y. Torisawa, E.I. Qendro and S. Lightbown for technical assistance, and R. Luna for helpful comments on the manuscript.

Author contributions

S.M., G.M.C. and D.E.I. conceived the strategy for this study; S.M. designed and performed experiments; S.M. and D.E.I. wrote the manuscript; T.M., T.C.F. and S.S.F.J. helped with the analysis of microscopy data; A.M. performed qPCR analysis; scanning electron microscopy analysis was performed by K.R., T.F.-D., S.K. and J.C.W.; M.H.-K. performed western blot experiments and analysed the data; S.C. performed LDH-release assay; S.M. and S.S.F.J. performed drug toxicity studies and analysed the data; R.N. and M.I. designed the microfluidic chips and built the programmable vacuum regulators. All authors discussed the results and commented on the manuscript.

Additional information

Supplementary information is available for this paper.

Reprints and permissions information is available at www.nature.com/reprints.

Correspondence and requests for materials should be addressed to D.E.I.

How to cite this article: Musah, S. *et al.* Mature induced-pluripotent-stem-cell-derived human podocytes reconstitute kidney glomerular-capillary-wall function on a chip. *Nat. Biomed. Eng.* **1**, 0069 (2017).

Publisher's note: Springer Nature remains neutral with regard to jurisdictional claims in published maps and institutional affiliations.

Competing interests

D.E.I. and S.M. are authors on a pending patent for methods for the generation of kidney glomerular podocytes from pluripotent stem cells (US patent application 14/950859). D.E.I. is a founder of Emulate, Inc., holds equity in it, and chairs its scientific advisory board.